Models for non-Newtonian flowback in an elastic fracture

A. Lenci, Università di Bologna, 40136 Bologna, Italy
V. Ciriello, Università di Bologna, 40136 Bologna, Italy
L. Chiapponi, Università di Parma, 43124 Parma, Italy
S. Longo, Università di Parma, 43124 Parma, Italy
V. Di Federico, Università di Bologna, 40136 Bologna, Italy

Key words: fractured media, elastic wall, non-Newtonian, experiments

Introduction

Flowback of fracturing fluid is an issue of considerable interest for its technical, economical [1] and environmental [2] implications. During hydrofracturing, a network of fractures and cracks is created; when the injection stops, the pressure in the stimulated zone drops, and the elastic relaxation of fluid-driven fractures drives the fracturing fluid and the proppant back towards the wellbore [3]. A conceptual model to represent the relaxation of a single planar fracture under flowback was first presented by [4]; the model was modified to account for converging flow in radial fractures by [5], who considered a fluid of power-law behavior to account for the typical non-Newtonian rheology of fracturing fluids [6]. Here, we present the main results for power-law fluid flowback in a radial fracture, and their extension in two respects, i.e. a planar geometry and the adoption of the Ellis rheological law to describe the fluid. The adoption of a three-parameter rheological model allows to describe more accurately the fluid behaviour at low shear rates.

Model formulation

We consider plane or annular circular fractures with planar walls. The layout for a radial fracture is represented in Fig. 1.

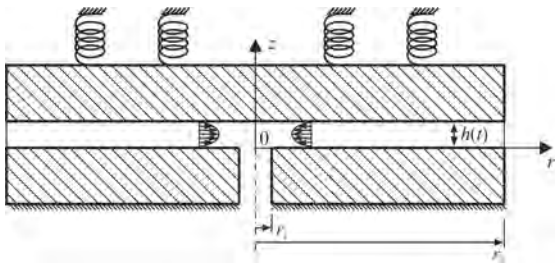

Figure 1: Layout of a radial fracture of internal radius r_i and external radius r_e; the fracture wall is constrained by elastic forces increasing with the aperture $h(t)$.

The walls are taken to be indeformable, and the relaxation phenomenon is represented via an elastic wall constrained by elastic forces increasing with the time-varying aperture $h(t)$. The fracture lies in a vertical plane perpendicular to a horizontal borehole or in a horizontal plane perpendicular to a vertical borehole. At time $t = 0$, the pressure p_e at the outlet r_i starts acting, the wall elastic response squeezes the fluid and forces a backflow towards the outlet as a consequence of the no-flow boundary condition at r_e. Gravity effects are absent in horizontal fractures and negligible with respect to pressure gradients for fractures in any other plane. The flow is viscous and the lubrication approximation is adopted. The rheological equation valid in simple shear flow $\tau_{zr} = -\mu(\partial u/\partial z)^n$ (with τ_{zr} shear stress, u velocity, μ consistency index and n flow behavior index) is coupled with the flow and mass balance equations and with the force balance on the fracture, reading

$$2\pi \int_{r_i}^{r_e} rp(r,t)\mathrm{d}r = \hat{E}\pi r_e^2 h^\lambda(t) + f_0, \tag{1}$$

where $\hat{E}$ is the effective spring constant of the wall, λ a positive dimensionless constant, and f_0 the overload. The formulation for the plane fracture is similar with obvious differences due to geometry.

Solution and results

Aperture and pressure fields. For both geometries, the problem is solved in dimensionless form yielding a nonlinear ODE for the fracture aperture, from this the pressure field along the fracture, the residual volume of fluid within it, and the outflow rate are easily obtained. The solution is analytical for zero exit pressure and

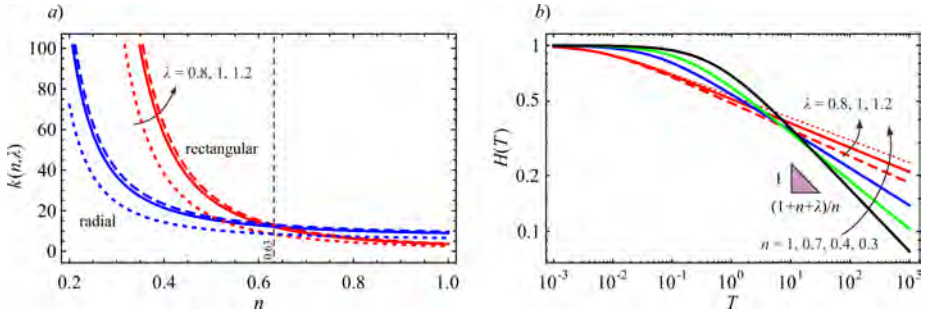

Figure 2: *a*) Decay ratio for linear and point drainage within a rectangular (plane) and a circular fracture, respectively. The curves refer to softening (dotted), linear (continuous) and stiffening (dashed) array of springs model. *b*) Dimensionless aperture as a function of time T for different values of flow behaviour index n and fracture wall constant λ. Dashed, continuous and dotted lines refer to $\lambda = 0.8, 1, 1.2$.

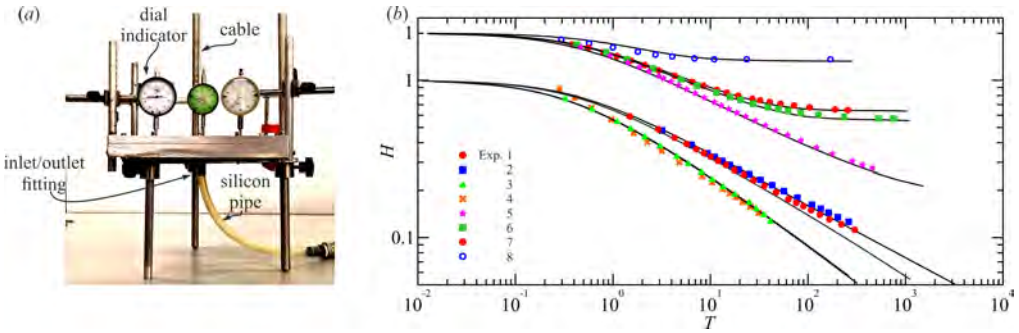

Figure 3: *a*) The experimental apparatus, and *b*) comparison between experiments (symbols) and theory (curves).

overload, e.g. the aperture field is given by $H(T) = [1 + k(n, \lambda)T]^{-n/(1+n+\lambda)}$, where the dependence on the drainage mechanism can be encapsulated in a decay coefficient $k(n, \lambda)$ for the fracture aperture, with $1/k$ being the dimensionless time scale of decay. Figure 2a depicts the behavior of $k(n, \lambda)$, showing the behavior of the decay rate as a function of n and λ. The late-time dependance of the aperture follows a $T^{-n/(n+\lambda+1)}$ power-law scaling with time T, an example is shown in Fig. 2b.

Ellis rheological model. We propose a generalization of the approach to Ellis rheology, being defined by an apparent viscosity of the fluid given by

$$\mu_{app} = \frac{\mu_0}{1 + (\tau/\tau_0)^{\alpha-1}} \ , \tag{2}$$

featuring three parameters, a viscosity μ_0, a constant τ_0 defined as the shear stress corresponding to apparent viscosity $\mu_0/2$, and an exponent α. The models are validated against experiments.

Experimental verification

The validation of model results was performed with an ad hoc apparatus in the Hydraulic Laboratory of Parma University, shown in Figure 3a. Twelve tests were conducted with a variety of parameters combinations, eight with Newtonian and four with shear-thinning fluids; the fracture apertures ranged from 0.90 to 1.20 mm; five tests had a nonzero exit pressure, with values ranging from 750 to 4740 kPa; two different values of the elastic constant $\hat{E}$ were employed; in three tests, an overload was present. The comparison between theory and experiments for some tests is shown in Figure 3b. Uncertainty quantification was also performed.

References

[1] Nolen-Hoeksema, R. (2013), Elements of hydraulic fracturing, *Oilfield Review*, *25(2)*, 51–52.

[2] Birdsell, D., H. Rajaram, and D. D. H. Viswanathan (2015), Hydraulic fracturing fluid migration in the subsurface: a review and expanded modeling results, *Water Resources Research*, *37*, 1–30.

[3] Medina, R., R. Detwiler, R. Prioul, W. Xu, and J. Elkhoury (2018), Settling and mobilization of sand-fiber proppants in a deformable fracture, *Water Resources Research*, *54*, 9964–9977.

[4] Dana, A., Z. Zheng, G. G. Peng, H. A. Stone, H. E. Huppert, and G. Z. Ramon (2018), Dynamics of viscous backflow from a model fracture network, *Journal of Fluid Mechanics*, *836*, 828–849.

[5] Chiapponi, L., V. Ciriello, S. Longo, and V. Di Federico (2019), Non-Newtonian backflow in an elastic fracture, *Water. Resour. Res.*, *55*, 1–15.

[6] Barbati, A., J. Desroches, A. Robisson, and G. McKinley (2016), Complex Fluids and Hydraulic Fracturing, *Annu. Rev. Chem. Biomol. Eng.*, *7*, 415–453.